Journal of Pharmaceutical and Biomedical Analysis 173 (2019) 1–17

Contents lists available at ScienceDirect

Journal of Pharmaceutical and Biomedical Analysis

journal homepage: www.elsevier.com/locate/jpba

Isotopic dilution method for bile acid profiling reveals new sulfate glycine-conjugated dihydroxy bile acids and glucuronide bile acids in serum

Maria M. Ulaszewska [a,*], Andrea Mancini [a], Mar Garcia-Aloy [a], Massimo Del Bubba [b], Kieran Micheal Tuohy [a], Urska Vrhovsek [a]

[a] Department of Food Quality and Nutrition, Research and Innovation Centre, Fondazione Edmund Mach (FEM), Via Mach 1, 38010, San Michele all'Adige, Trento, Italy
[b] Department of Chemistry, University of Florence, Via della Lastruccia 3, 50019, Sesto Fiorentino, Florence, Italy

ARTICLE INFO

Article history:
Received 29 January 2019
Received in revised form 2 April 2019
Accepted 2 May 2019
Available online 9 May 2019

Keywords:
Bile acids
Profiling
Postprandial kinetics
Metabotypes
Triple Quad
Orbitrap

ABSTRACT

An ultrahigh performance liquid chromatography tandem mass spectrometry method (UHPLC-MS/MS) was developed for the determination of 41 target and 8 additional bile acids isomers (BAs) in biological fluids. BAs were analysed by solid-phase extraction on 50 μL biofluid-aliquots, followed by a properly optimised 27 min-chromatographic run. The method provided high sensitivity (limits of detection 0.0002–0.03 μM, limits of quantitation 0.0007–0.11 μM), linearity (R^2>0.99) and precision (relative standard deviations ≤16%). A strategy of scheduled/ unscheduled injections of real samples together with neutral loss (80 Da and 176 Da) scans allowed us to find additional bile acid isomers not *a priori* included in the method, while high resolution full scan and MS/MS fragmentation analysis confirmed their structural adherence to the bile acid family. Moreover this is the first study quantifying four sulfate glycine conjugated-dihydroxy bile acid isomers, independently of the diet and postprandial time. Application to a dietary intervention kinetic study confirmed the existence of possible metabotypes amongst the study population (n = 20). A trend differentiating males from females was observed suggesting that serum samples from women contained smaller amounts of certain bile acids.

1. Introduction

Bile acids (BAs) are derived from cholesterol metabolism. Chemically they are saturated, hydroxylated C-24 cyclopentanephenanthrene sterols and they are the major functional component of bile. At the hepatocyte level, starting from cholesterol and through cytochrome P450 family enzymes such as CYP7A1, CYP8B1 and CYP27A1 [1,2], two primary BAs are synthetized, namely cholic acid and chenodeoxycholic acid. These are subsequently conjugated by bile acid cholyl-CoA synthetase and acid-CoA: amino acid N-acyltransferase with glycine and/or taurine and then stored in the gall bladder before being released into the small intestine [1–3]. Recent investigations shown that BAs concentration in postprandial OGTT challenge rich maximum values already within 30 min up to 1 h, what suggest that BAs can be absorbed already in the upper part of the small intestine [4]. Beside of taurine and glycine, BAs can be conjugated also as sulfated metabolites or with N-acetyl glucosamine, glutathione, glucose or glucuronate [5–7]. See scheme on Fig. 1 for detailed description of bile acid structures, and primary and secondary metabolism routes. Gut microbiota has a strong influence in regulating the BA pool. Perturbations in gut microbiota community structure can induce significant changes in BAs profiles and concentrations entering the enterohepatic circulation and influence BA cell signaling in the host. Indeed, secondary BA derived from microbial metabolism in the gut play a regulatory role in the synthesis of BA in the liver through farnesoid X receptor (FXR), G protein-coupled receptor (TGR5) and fibroblast growth factor (FGF-19) signaling. Diet:gut microbiota interactions therefore are likely to play a key role in influencing both hepatic BAs neosynthesis and production of secondary and tertiary BAs in the intestine [1,8–11]. However, there are few studies exploring how diet:microbe interactions can modulate BAs profile in human. Probiotic bile salt hydrolase activities [9], polyphenols and prebiotic fibers like oat β-glucans [12,13] has been shown to modulate the gut microbiota composition and consequently the BA pool. On the other hand certain fibers as β-glucans/oats, apple pectin, proanthocyanidins or condensed tannins, may sequester BAs, driving them distally into the

* Corresponding author.
E-mail address: maria.ulaszewska@gmail.com (M.M. Ulaszewska).

https://doi.org/10.1016/j.jpba.2019.05.002

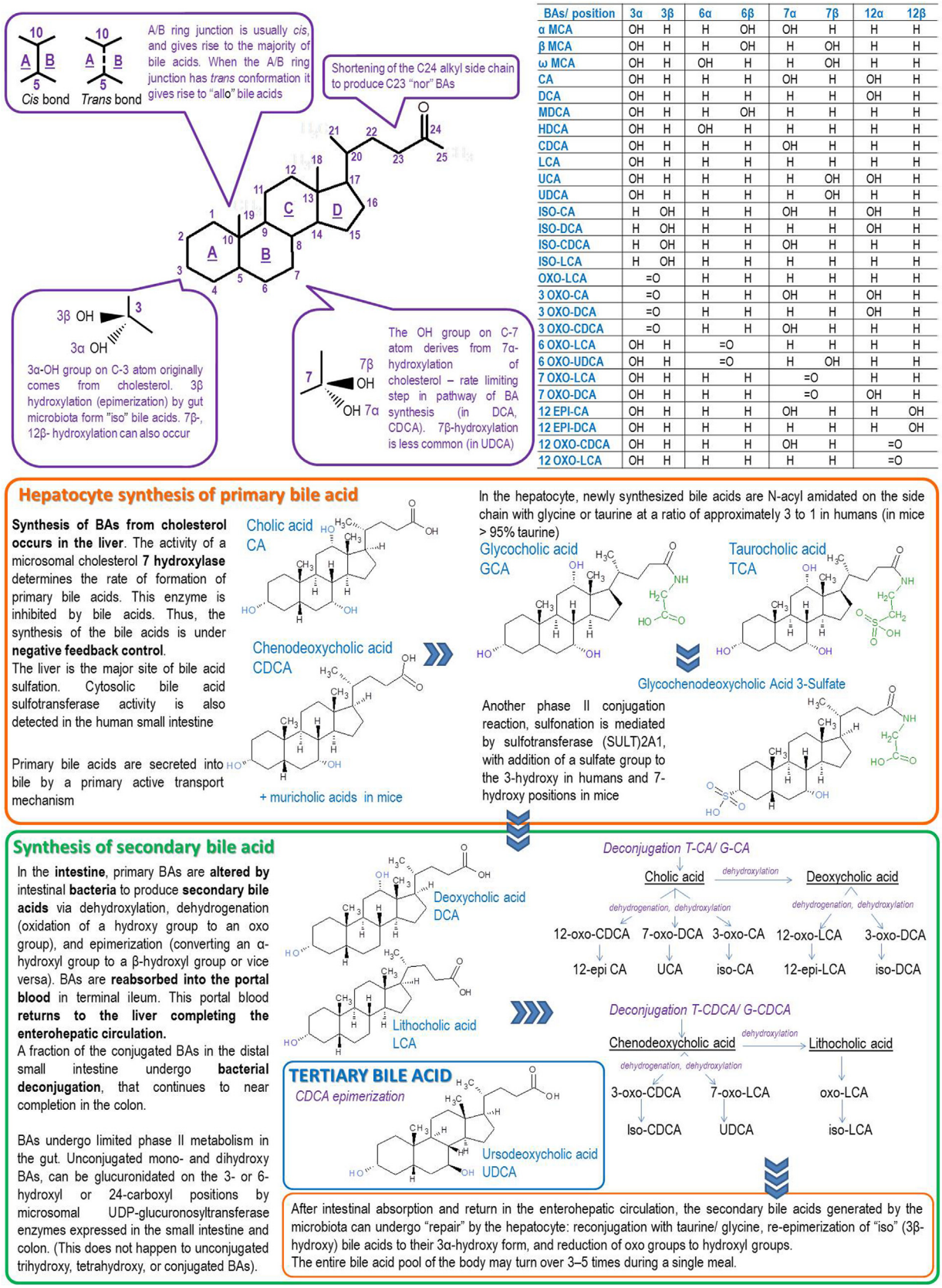

BAs/ position	3α	3β	6α	6β	7α	7β	12α	12β
α MCA	OH	H	H	OH	OH	H	H	H
β MCA	OH	H	H	OH	H	OH	H	H
ω MCA	OH	H	OH	H	H	OH	H	H
CA	OH	H	H	H	OH	H	OH	H
DCA	OH	H	H	H	H	H	OH	H
MDCA	OH	H	H	OH	H	H	H	H
HDCA	OH	H	OH	H	H	H	H	H
CDCA	OH	H	H	H	OH	H	H	H
LCA	OH	H	H	H	H	H	H	H
UCA	OH	H	H	H	H	OH	OH	H
UDCA	OH	H	H	H	H	OH	H	H
ISO-CA	H	OH	H	H	OH	H	OH	H
ISO-DCA	H	OH	H	H	H	H	OH	H
ISO-CDCA	H	OH	H	H	OH	H	H	H
ISO-LCA	H	OH	H	H	H	H	H	H
OXO-LCA	=O		H	H	H	H	H	H
3 OXO-CA	=O		H	H	OH	H	OH	H
3 OXO-DCA	=O		H	H	H	H	OH	H
3 OXO-CDCA	=O		H	H	OH	H	H	H
6 OXO-LCA	OH	H	=O		H	H	H	H
6 OXO-UDCA	OH	H	=O		H	OH	H	H
7 OXO-LCA	OH	H	H	H	=O		H	H
7 OXO-DCA	OH	H	H	H	=O		OH	H
12 EPI-CA	OH	H	H	H	OH	H	H	OH
12 EPI-DCA	OH	H	H	H	H	H	H	OH
12 OXO-CDCA	OH	H	H	H	OH	H	=O	
12 OXO-LCA	OH	H	H	H	H	H	=O	

Fig. 1. Scheme representing bile acids structures, primary bile acids and secondary bile acids synthesis and transformations in different body compartments.

colon where they may be excreted or transformed by the resident microbiota into secondary BAs or modified chemical structures [14].

Due to the involvement of specific BAs in various regulatory processes, increasing attention and efforts have been given to develop methodologies for their profiling and accurate quantification in

Table 1
Mass spectrometry parameters for bile acids included in the quantification method reported in order according di increasing Precursor ion value, and increasing retention time.

No	Compounds	Rt in min	Ionization Mode	Precursor ion	Q1 – quantifier				Q2 – qualifier				
					Product Ion	DP	CE	CXP	Precursor ion	Product Ion	DP	CE	CXP
1	Lithocholic acid	21.41	[M−H]-	375.3	375.3	−145	−18	−10	375.3	357.3	−270	−46	−27
2	6-Ketolithocholic acid	14.30	[M−H]-	389.3	389.3	−150	−18	−10	389.3	327.3	−230	−44	−19
3	7-Ketolithocholic acid	15.06	[M−H]-	389.3	389.3	−255	−40	−17	389.3	343.3	−240	−48	−9
4	12-Ketolithocholic acid	15.47	[M−H]-	389.3	389.3	−255	−40	−17	389.3	343.3	−230	−42	−23
–	Ketolithocholic acid (isomer 1)	16.06	[M−H]-	389.3	389.3	−255	−40	−17	389.3	343.3	−230	−42	−23
–	Ketolithocholic acid (isomer 2)	17.43	[M−H]-	389.3	389.3	−255	−40	−17	389.3	343.3	−230	−42	−23
5	Murocholic acid	12.01	[M−H]-	391.3	391.3	−150	−18	−10	391.3	373.3	−245	−44	−23
6	Ursodeoxycholic acid	13.36	[M−H]-	391.3	391.3	−150	−18	−10	391.3	373.3	−280	−48	−25
7	Hyodeoxycholic acid	13.61	[M−H]-	391.3	391.3	−150	−8	−10	391.3	373.3	−280	−48	−25
8	Chenodeoxycholic acid	16.95	[M−H]-	391.3	391.3	−150	−18	−10	391.3	373.3	−280	−48	−25
9	Deoxycholic acid	17.40	[M−H]-	391.3	391.3	−150	−18	−10	391.2	345.2	−125	−46	−10
10	Dehydrocholic acid	8.37	[M−H]-	401.2	401.2	−255	−40	−17	401.2	331.2	−225	−36	−23
11	7-dehydrocholic acid	10.01	[M−H]-	405.3	405.3	−200	−18	−10	405.2	289.2	−235	−48	−19
12	Ursocholic acid	7.45	[M−H]-	407.3	407.3	−166	−18	−10	407.3	343.3	−130	−46	−11
13	α-Muricholic acid	9.60	[M−H]-	407.3	407.3	−166	−18	−10	407.3	387.3	−250	−50	−10
14	β-Muricholic acid	10.22	[M−H]-	407.3	407.3	−166	−18	−10	407.3	371.2	−270	−48	−23
15	Hyocholic acid	11.56	[M−H]-	407.3	407.3	−166	−18	−10	407.3	389.3	−255	−46	−25
16	Allocholic acid	12.70	[M−H]-	407.3	407.3	−166	−18	−10	407.3	343.3	−130	−46	−11
17	Cholic acid	12.82	[M−H]-	407.3	407.3	−125	−30	−29	407.3	345.3	−300	−42	−23
18	Glycolithocholic acid	17.88	[M−H]-	432.3	74.1	−118	−66	−10	432.3	388.3	−120	−46	−10
19	Glycoursodeoxycholic acid	9.26	[M−H]-	448.3	74.1	−125	−70	−10	448.3	386.3	−132	−49	−12
20	Glycohyodeoxycholic acid	9.53	[M−H]-	448.3	74.1	−120	−69	−10	448.3	386.3	−132	−49	−12
21	Glycochenodeoxycholic acid	13.50	[M−H]-	448.3	74.1	−106	−69	−10	448.3	386.3	−132	−49	−12
22	Glycodeoxycholic acid	14.20	[M−H]-	448.3	74.1	−106	−69	−10	448.3	404.3	−125	−44	−10
23	Lithocholic acid -3-*O*-sulfate	17.20	[M−H]-	455.2	96.9	−185	−50	−9	455.2	80	−185	−122	−9
24	Glycodehydrocholic acid	4.71	[M−H]-	458.3	74.1	−120	−71	−10	458.3	414.3	−120	−40	−10
25	Glycohyocholic acid	7.90	[M−H]-	464.3	464.3	−120	−16	−29	464.3	74.1	−125	−70	−10
26	Glycocholic acid	9.43	[M−H]-	464.3	464.3	−120	−16	−29	464.3	74.1	−125	−70	−10
27	Taurolithocholic acid	15.85	[M−H]-	482.3	482.3	−175	−16	−17	482.3	80	−150	−123	−10
28	Cholic acid – 7-*O*-sulfate	8.74	[M−H]-	487.2	79.9	−185	−130	−13	487.2	97.1	−185	−36	−11
29	Tauroursodeoxycholic acid	6.87	[M−H]-	498.3	498.3	−180	−14	−17	498.3	79.9	−150	−123	−10
30	Taurohyodeoxycholic acid	7.03	[M−H]-	498.3	498.3	−180	−14	−17	498.3	79.9	−150	−123	−10
31	Taurochenodeoxycholic acid	10.91	[M−H]-	498.3	498.3	−180	−14	−17	498.3	79.9	−150	−123	−10
32	Taurodeoxycholic acid	11.77	[M−H]-	498.3	498.3	−180	−14	−17	498.3	79.9	−150	−123	−10
33	Tauro ω muricholic acid	3.45	[M−H]-	514.3	514.3	−180	−18	−19	514.3	80	−180	−124	−10
34	Tauro α muricholic acid	3.80	[M−H]-	514.3	514.3	−180	−18	−19	514.3	80	−180	−124	−10
35	Tauro β muricholic acid	4.01	[M−H]-	514.3	514.3	−180	−18	−19	514.3	80	−180	−124	−10
36	Taurohyocholic acid	5.64	[M−H]-	514.3	514.3	−180	−18	−19	514.3	80	−180	−123	−10
37	Taurocholic acid	9.26	[M−H]-	514.3	514.3	−180	−18	−19	514.3	80	−180	−123	−10
–	Glycoursodeoxycholic acid sulfate	5.57	[M−H]-	528.2	448.3	−140	−44	−33	528.2	97.1	−140	−112	−9
–	Glyco-dihydroxy bile acid sulfate	6.49	[M−H]-	528.2	448.3	−140	−44	−33	528.2	97.1	−140	−112	−9
38	Glycochenodeoxycholic acid-3-*O*-sulfate	9.60	[M−H]-	528.2	448.3	−140	−44	−33	528.2	97.1	−140	−112	−9
–	Glycodeoxycholic acid sulfate	9.94	[M−H]-	528.2	448.3	−140	−44	−33	528.2	97.1	−140	−112	−9
39	Taurolithocholic acid -3-*O*-sulfate	12.73	[M−H]-	562.2	482.1	−170	−34	−33	562.2	80.1	−170	−130	−7
–	Dihydroxy bile acid glucuronide (isomer 1)	9.17	[M−H]-	567.3	391.2	−130	−58	−25	567.3	75.1	−130	−80	−9
–	Dihydroxy bile acid glucuronide (isomer 2)	9.58	[M−H]-	567.3	391.2	−130	−58	−25	567.3	75.1	−130	−80	−9
40	Chenodeoxycholic acid-3-β-glucuronide	12.97	[M−H]-	567.3	391.2	−130	−58	−25	567.3	75.1	−130	−80	−9
–	Dihydroxy bile acid glucuronide (isomer 3)	13.20	[M−H]-	567.3	391.2	−130	−58	−25	567.3	75.1	−130	−80	−9
–	Dihydroxy bile acid glucuronide (isomer 4)	13.57	[M−H]-	567.3	391.2	−130	−58	−25	567.3	75.1	−130	−80	−9
41	Taurocholic acid-3-*O*-sulfate	5.01	[M−H]-	594.2	514.2	−110	−34	−37	594.2	80	−110	−130	−9
42	Lithocholic acid d4	21.41	[M−H]-	379.3	379.3	−135	−18	−10					
43	Deoxycholic acid d4	11.40	[M−H]-	395.3	395.3	−150	−18	−10	395.2	349.3	−235	−46	−19
44	Ursodeoxycholic acid d4	13.36	[M−H]-	395.3	395.3	−150	−18	−10	395.2	349.3	−235	−46	−19
45	Chenodeoxycholic acid d4	16.95	[M−H]-	395.3	395.3	−150	−18	−10	395.3	349.3	−235	−46	−19

Table 1 (*Continued*)

No	Compounds	Rt in min	Ionization Mode	Precursor ion	Q1 – quantifier				Q2 – qualifier				
					Product Ion	DP	CE	CXP	Precursor ion	Product Ion	DP	CE	CXP
46	Cholic acid d4	12.82	[M−H]-	411.3	411.3	−140	−18	−10	411.3	347.3	−130	−46	−11
47	Glycolithocholic acid d4	17.88	[M−H]-	436.3	74.1	−120	−66	−10	436.3	436.3	−120	−16	−13
48	Glycoursodeoxycholic acid d4	9.26	[M−H]-	452.2	74.1	−125	−69	−10	452.3	390.3	−180	−50	−23
49	Glycochenodeoxycholic acid d4	13.50	[M−H]-	452.4	74.1	−125	−69	−10	452.3	390.3	−180	−50	−23
50	Glycocholic acid d4	9.43	[M−H]-	468.3	74.1	−120	−73	−10	468.2	406.3	−200	−50	−23
51	Taurolithocholic acid –d5	15.85	[M−H]-	487.2	79.9	−150	−123	−9	487.2	123.9	−285	−66	−9
52	Taurochenodeoxycholic-d5	10.91	[M−H]-	503.3	79.9	−150	−123	−10	503.4	503.3	−180	−14	−17
53	Taurodeoxycholic acid-d5	11.77	[M−H]-	503.3	80	−150	−123	−10	503.3	503.3	−180	−14	−17
54	Taurocholic acid-d5	7.43	[M−H]-	519.3	80	−180	−100	−13	519.3	124.1	−180	−68	−9
55	Glycochenodeoxycholic acid-d5-3-sulfate	9.60	[M−H]-	533.1	453.3	−235	−46	−33	533.1	98.1	−235	−130	−13
56	Hippuric Acid d5 (External Standard)	1.20	[M−H]-	182.9	139.2	−75	−16	−9	182.9	82.1	−75	−24	−11

various biological samples such as bile, feces, serum, plasma and urine [15,16]. However separation and quantification of individual BAs and their derived metabolites, represent the major challenge due to wide differences in their physicochemical properties, their complex structure, their low concentration in some matrices and existence of multiple isomeric forms [6,3]. Generally, in the healthy condition, plasma BAs, represent the balance between intestinal input and hepatic contribution. Urinary BAs represent filtered BAs plus any BAs secreted by the tubules. In feces, BAs represent BA residual not reabsorbed from the intestine [3]. It follows that the majority of bile acids are in the biliary tract and intestine, while plasma and urine levels are low (<10 μM) [3,17].

Serum BAs identification and quantification can be based on different methods [18–20]., however liquid chromatography–tandem mass spectrometry (LC–MS/MS) represent the main approach in the analysis of free and conjugated BAs in biological samples and also the sulfates derivatives [17,20,21,15,22,19,6]. An important issue in quantification of bile acids is difficulty in obtaining matrix (plasma, serum, or tissues) free of their content. It is well known that matrix effects may affect signal intensities in electrospray ionization (ESI) and thus is considered as a main challenge for reliable quantitative LC–MS/MS. Since in case of endogenous compounds a complete removal of matrix effect is rather not possible, internal standards (ISs) are added to address matrix effects issue and allow for reliable quantification by LC–ESI-MS/MS. Stable isotope labelled internal standards are considered the gold standard because they closely resemble the properties of the analyte and show similar ionization efficiencies and retention times [23]. Since matrix effects is not uniform as a function of retention time and can vary substantially between different samples, only ISs co-eluting with the analyte can compensate these variations. Thus, in this work we present an isotopic dilution LC–ESI-MS/MS method for a comprehensive analysis of BAs in human serum and plasma with application to kinetic study with *Vaccinium corymbosum* (VC) and *Vaccinium myrtillus* (VM). We used a combination of quantitative (LC-Triple Quad) and qualitative (LC-HR-Orbitrap) analysis for discovery of BAs isomers. Their presence was confirmed thanks to fragmentation pattern similarities with analytical standards and mass accuracy measurements in full scan and MS/MS modes.

2. Experimental section

2.1. Materials

LC–MS grade acetonitrile, methanol, formic acid, were obtained from Sigma-Aldrich. Ostro 96 well plates for phospholipid retention were purchased from Waters. The authentic compounds of 20 unconjugated, 9 glycine conjugated, and 12 taurine conjugated bile acids as well as labelled with deuterium bile acid and hippuric acid d5 were ordered from Spectra 2000s.r.l, Cabru s.r.l, and Sigma Aldrich (See Supplementary Table 1 for details). Human plasma and human serum were ordered from Sigma Aldrich. Names and abbreviations for bile acids are given in Table 1 and Supplementary Table 1.

Standard solutions and calibration curves. Stock mother solutions (concentration ranged between 1400 ppm–15000 ppm) of bile acids were individually prepared from their authentic compounds in pure methanol. These stock solutions were further diluted with methanol to give 100 ppm solutions of each bile acid, and to make a mix of native compounds in pure methanol with concentration between 50–150 μM. Stability of compounds in pure methanol stored in −80 °C last for approximately one year, while working solutions on Methanol/Water (1:1 v/v) for approximately 6 months. This standard solution was used for preparation of calibration curves and for determination of the limits of detection (LODs)

and limits of quantitation (LOQs). Labelled with deuterium bile acids were prepared in similar way, with final mix solution in pure methanol with concentration of 2 μM. Calibration curves in human plasma, human serum and solvent (methanol/water 1:1) covered wide range of concentrations: 0.0005 μM – 5 μM. Considering that matrix free from bile acids does not exist, isotopic dilution method was used for reliable quantification of these compounds. Validated method was applied to serum samples from an intervention study where twenty healthy volunteers consumed two types of berry supplements: 25 g of *Vaccinium corymbosum* (VC) powder or 25 g of *Vaccinium myrtillus* (VM) powder, each administered with 500 mL of water. Serum samples were collected at baseline and different sampling times: 30, 60, 120, 240 and 360 min after the supplement assumption (Ethical approval for the administration was obtained for a phase I-II study: approval n. SPE 14.178 AOUC, 30th May 2016)

2.2. Extraction method

Plasma and serum samples were extracted with method descried elsewhere [16]. Blood samples have a high content of phospholipids. As shown by Han et al, their removal by phospholipid depletion solid phase extraction (PD-SPE), based on the Lewis acid–base interactions mechanism, helps to reduce matrix effects in LC–ESI-MS analysis. Thus Ostro 96 well plates by Waters were used for plasma and serum extraction. Briefly, 50 μL of plasma or serum were loaded onto Ostro 96well plate, together with internal standard solution consisting of known amount deuterated bile acids (0.15 μM - 0.3 μM), followed by 150 μL of cold acetonitrile with 1% of formic acid. Samples were filtered using positive pressure-96 manifold (Waters, USA). Additionally the filtering plate was eluted with second portion of 150 μL of cold acetonitrile with 1% of formic acid. Samples were evaporated with gentle stream of nitrogen to dryness using a Techne Dr-block DB 3D heater at room temperature and re-dissolved with 100 μL of water: methanol (1:1 V/V).

2.3. UHPLC–MRM-MS

Chromatographic separation of the compounds was made using the Zorbax Eclispe XDB-C18 (Agilent) 2.1 × 100 mm, 1.8 μm with pre-column 4.0 mm x 2.0 mm I.D (Phenomenex Torrance, CA, USA). A triple quadrupole mass spectrometer system (5500 Triple Quad AB Sciex Instruments, Foster City, CA, USA) with an electrospray ionization (ESI) source coupled to a Dionex UHPLC system was used for analysis of metabolites. The flow rate was 450 μl/min and column temperature was maintained at 40 °C. Mobile phases used were: Milli-Q water (Solvent A), acetonitrile (Solvent B), both with 0.1% formic acid (all solvents of LC–MS grade). Elution gradient based on previously developed by Han et al, [16] with small modifications: 0–1.5 min 25% of solvent B, increase form 1.5 min–12 min up to 40% of solvent B; followed by further increase 12 min–14 min up to 75% solvent B, and 14 min–25 min increase up to 100% solvent B. Keep 100% of solvent B for two minutes. Decrease up to 75% solvent B in 0.1 min, and keep until 27 min. Injection volume was of 5 μL. The ESI setting parameters were: the source temperature was set at 600 °C, ion source voltage -4500, the nebulizer gas (Gas1) and heater gas (Gas2) at 40 and 50 psi respectively (1 psi =6894.76 Pa). UHPLC nitrogen (99.999%) was used as both curtain (CUR) and collision gas (CAD) at 35 and 10 psi respectively. Nitrogen was used as the nebulizer gas, curtain gas and collision gas. The two most abundant fragments to use as quantifier and qualifier were identified for each compound. Declustering potential (DP) and entrance potential (EP) were optimised for each precursor ion and collision energy (CE) and collision cell exit potential (CXP) for each product ion by direct infusion of analytical standards. Table 1 contains the compound-specific instrumental parameters used in the analytical method.

2.4. HPLC–Orbitrap MS

High resolution MS and MSn spectra were obtained from hybrid linear ion trap Fourier Transform (LTQ FT) Orbitrap HR-MS (Thermo Fisher, Bremen, Germany) with an electrospray ionization (ESI) operating in positive and negative ionization modes. The MS system was coupled with a Dionex Ultimate 3000 HPLC system equipped with an Zorbax Eclispe XDB-C18 (Agilent) 2.1 × 100 mm, 1.8 μm with pre-column 4.0 mm x 2.0 mm I.D (Phenomenex Torrance, CA, USA). Chromatographic conditions were similar to the one set for targeted experiments, except from mobile phase flow which was lower due to differences in binary pumps. Samples were injected in DDA mode consisting of full scan event followed by three MS/MS scan events for selected *m*/*z* feature: here bile acid of our interest. Full scan event covered mass range from 100 to 600 Da at a mass resolution of 30,000 FWHM (full width at half maximum for *m*/*z* 400) in centroid mode. Three consecutive MS/MS events were operating under 7500 resolution. Product ions were generated in the LTQ trap at collision energy 35 eV using an isolation width of 1 Da.

3. Statistics

The analyses were performed using the R software (version 3.5.1). From statistical analysis following compounds were excluded dehydroCA, G-dehydroCA, AlloCA, β-MCA, UrsoCA, T-HDCA, T-β-MCA, HDCA, MuroCA, T-CA-SULF and CA-SULF, 6-KLCA, 12-KLCA, KLCA isomer (Rt 16.04 min), G-CDCA sulfate (isomer at Rt 6.49 min) as they were not detected in all study samples. Firstly, missing values (defined as those values below the limit of detection) were imputed using a random value between the percentile 2.5 and 5 of the limit of detection value for the corresponding metabolite. Principal component analysis (PCA) on log-transformed and Pareto-scaled data was applied to detect the presence of outliers and to check possible batch effect, as well as to assess potential associations among samples according to different characteristics of volunteers. Visualization of PCA results was performed using "factoextra" package. Postprandial response was evaluated through area under the curve (AUC). AUC values were computed using the trapezoid method included in "pracma" package. According to the number of groups compared, two independent sample *t*-test or one-way ANOVA was used. All tests were conducted on log-transformed data, where 2-sided and p-values < 0.05 were considered statistically significant. Hierarchical clustering was performed on log-transformed and Pareto-scaled data using Euclidean distances. Results are expressed as mean ± standard error.

4. Results and discussion

4.1. Optimization of MRM and search of additional bile acid isomers

Individual MS parameters for each bile acid were assessed by direct infusion, three most intensive MRM were selected for further injection with chromatographic column. Due to the fact that most of the bile acids, especially the unconjugated ones, do not fragment well, the most intensive signals were obtained with daughter ions having the same mass as the parent ions [18,24]. This signal was used as quantifier. For glycine conjugated bile acids, transition from parent ion to glycine moiety was the strongest signal, and therefore this signal was used as quantifier. The entrance potential was set to -10 for all compounds. Table 1 and Supplementary Table 2 show all bile acids native and labelled with corresponding MS parameters.

Thanks to the C18-reverse phase chromatography, the sulfo-conjugates, tauro-conjugates, glyco-conjugates and unconjugated

bile acids were eluted as a function of their hydrophilicity/hydrophobicity balance. Separation of isomers on LC column and their distribution along the retention time was verified. Five isomers of dihydroxy BAs (*m/z* 391.3) included in the method eluted in order: MuroCA (Rt=12.01 min) – UDCA (Rt = 13.36 min) – HDCA (Rt = 13.61 min) – CDCA (Rt = 16.95 min) - DCA (Rt=17.40 min). The same order of elution was found for glycine- and taurine- conjugated bile acids with only difference that glycine conjugated BAs eluted ca. 3 min earlier, while taurine conjugated BAs ca. 6 min earlier (See Table 1). Groups of trihydoxy-BAs (*m/z* 407.3) and tauro-trihydroxy BAs (*m/z* 514.3) consist of higher number of isomers, respectively six and five. Good separation for all of them was achieved with elution order: UCA (Rt =7.45 min) – α MCA (Rt =9.60 min) – β MCA (Rt =10.22 min) – HCA (Rt =11.56 min) – AlloCA (Rt =12.70 min) – CA (Rt =12.82 min) while tauro-trihydroxy BAs isomers eluted in order: T-ωMCA (Rt =3.45 min) - T-αMCA (Rt = 3.80) - T-βMCA (Rt = 4.01) – T-HCA (Rt = 5.64 min) – T-CA (Rt =9.26 min). Some recent papers develop techniques with short runs that separate only 13–18 species but do not include sulfate and glucuronide conjugated bile acids as in our case [24,25,20], while longer chromatographic runs allowed for analysis of higher numbers of bile acid species [6,26,18], moreover allow for additional introduction of novel isomers that may be discovered.

The distribution of bile acids along the retention time allowed us to assign putative names to additional isomers found in real samples. Bile acids are a wide family of metabolites and consist of many isomers. For this reason a series of real samples was injected in unscheduled mode to verify presence of additional isomers not initially included in the method. The declustering potential and collision energy voltages used were the mean values from the parameters for all isomeric members in each group. This unscheduled screening of real samples was performed including three structurally specific pairs of the Q1 to Q3 ion transitions, See Table 1 and Supplementary Materials Table 2. Further verification and confirmation of their presence in samples was performed through injection on LC-HR- Orbitrap MS, where high resolution mass spectra were acquired. These additional analyses in unscheduled mode brought a series of interesting outcomes. Three additional sulfate isomers of glycine conjugated-dihydroxy BAs (*m/z* 528.2) were found in human plasma and serum from Sigma Aldrich supplier, as well as in serum QC sample from our study. Thanks to characteristic isomer distribution on chromatogram two were assigned as glycodeoxycholic acid sulfate (Rt =9.94 min) and glycoursodeoxycholic acid sulfate (Rt =5.57 min). Name to the third isomer (Rt=6.49 min) was not assigned, however it might be glycohyodeoxycholic acid sulfate, considering elution near glycoursodeoxycholic acid sulfate, or other isomer where sulphate group was located at *O*-7 position. The MRM transitions and DP, CE, CEX parameters are given in Table 1. Further scan using neutral loss modality (80 Da) prove the presence of sulfate moiety for all above mentioned isomers. The same samples were injected on HR Orbitrap mass spectrometer to verify fragmentation of additionally found isomers, and to confirm their structural similarities to analytical standard of glycochenodeoxycholic acid sulfate. Fig. 2 shows four isomers and their retention times observed in Triple-Quad mass spectrometer (panel A), and the same isomers found in HR Orbitrap mass spectrometer with corresponding MS^2 spectra (panel B). Injection in latter instrument fully confirmed structural similarities with analytical standard of glycochenodeoxycholic acid 3-*O*-sulfate, as first main fragment of precursor ion *m/z 528.26 was m/z/z* 52,826 was *m/z* 448.3068 (sulfate moiety loss). Quantifier transition for all four isomers was the same, meaning 528.3/448.2. All isomers were quantified based on glycochenodeoxycholic acid 3-*O*- sulfate-d4 labelled standard, with following concentration trend starting from the most concentrated BA: glycochenodeoxycholic acid 3-*O*-sulfate followed by glycodeoxycholic acid sulfate, glycoursodeoxycholic acid sulfate and the fourth isomer. Except for a series of sulfate conjugated BAs, also glucuronide bile acids were found in plasma and serum samples: three isomers dihydroxy-BAs (*m/z* 567.3) at Rt =9.12 min, Rt =9.60 min, Rt =13.20 min, with structural similarities verified with analytical standard of chenodeoxycholic acid- 3*O*-β glucuronide (Rt =12.93 min) – see Supplementary Fig. 2. Also in this case a combination of injection with three different modalities (unscheduled MRM modality, neutral loss modality of 175 Da and high resolution MS) were performed.

In similar manner two additional isomers of ketolithocholic acid were found. Our method includes three isomers: 6-, 7- and 12-ketolithocholic acids, with retention times at 14.30 min, 15.06 min and 15.47 min, respectively. Two additional isomers were found at Rt =16.06 min and Rt =17.43 min, with three MRM transitions monitored along unscheduled run: 389/389, 389/343 and 389/327 characteristic to ketolithocholic acids. High resolution spectra in full scan and in MS/MS modes confirmed their presence based on mass accuracy of molecular ions and fragmentation ions. Fragmentation patterns for all five isomers are shown in Supplementary Fig. 3. Similarities between MS/MS spectra of standard solutions and additional isomers are observable, with four fragments repeating in all spectra: *m/z* 327.2546, *m/z* 343.2643, *m/z* 345.2440 and *m/z* 371.2637.

Based on research by Thakare et al [27], Han et al [16], and Huang et al [19] additional set of MRM transitions were added in unscheduled method to verify presence of tetrahydroxy biles acids, oxo-bile acids, and other sulfate conjugates of UDCA, CDCA, DCA, G-LCA, G-CA, T-UDCA, T-CDCA, T-DCA however none were found in the plasma and serum samples (See Supplementary Materials Table 3 for MRM conditions of additional screening).

4.2. Method validation

After optimization of MS parameters and inclusion of additional isomers in the MS method, an appropriate method validation was performed according to the currently accepted US Food and Drug Administration (FDA) bioanalytical method validation guide [28]. Validation assays were established on calibration standards and spiked samples prepared from human plasma and human serum from Sigma Aldrich. The linearity in the analytical response, the limits of detection and quantification (LODs and LOQs, respectively), repeatability and reproducibility were evaluated. Assessment of recoveries was done with use of deuterated standards added at three concentrations levels into serum samples: ca 0.1 μM, ca 1.0 μM and 2.0 μM and, different concentrations levels reflects variability of concentrations found in real samples, each concentration level was repeated 3 times. Serum was also used to evaluate the intra- and inter-day variability, and were obtained from the repeated analysis (n = 5) of analytes over 1 day and 5 days, respectively, see Supplementary Tables 2–4 for details. To assess linearity solvent and matrix-matched calibration curves were prepared by spiking human plasma and human serum extracts at different concentration levels from ca 0.0005 μM – ca 5.0 μM (See Table 2 for details for each bile acid). The degree of enhancement or suppression due to the matrix effect was calculated as follow: ((solvent slope)/(matrix slope)*100 – 1). In such context, a negative result indicates ionization suppression, whereas a positive result indicates signal enhancement. The limits of quantification (LOQ) and limits of detection (LOD) were evaluated in solvent at the concentration in which the quantifier transition presented a signal to noise (S/N) ratio of >10 and >3 respectively (Table 2). Quantitative analyses were performed based in isotopic dilution method, where known amount of deuterated bile acids was added before extraction. Deuterated hippuric acid-d5 was used as external standard to account for recovery.

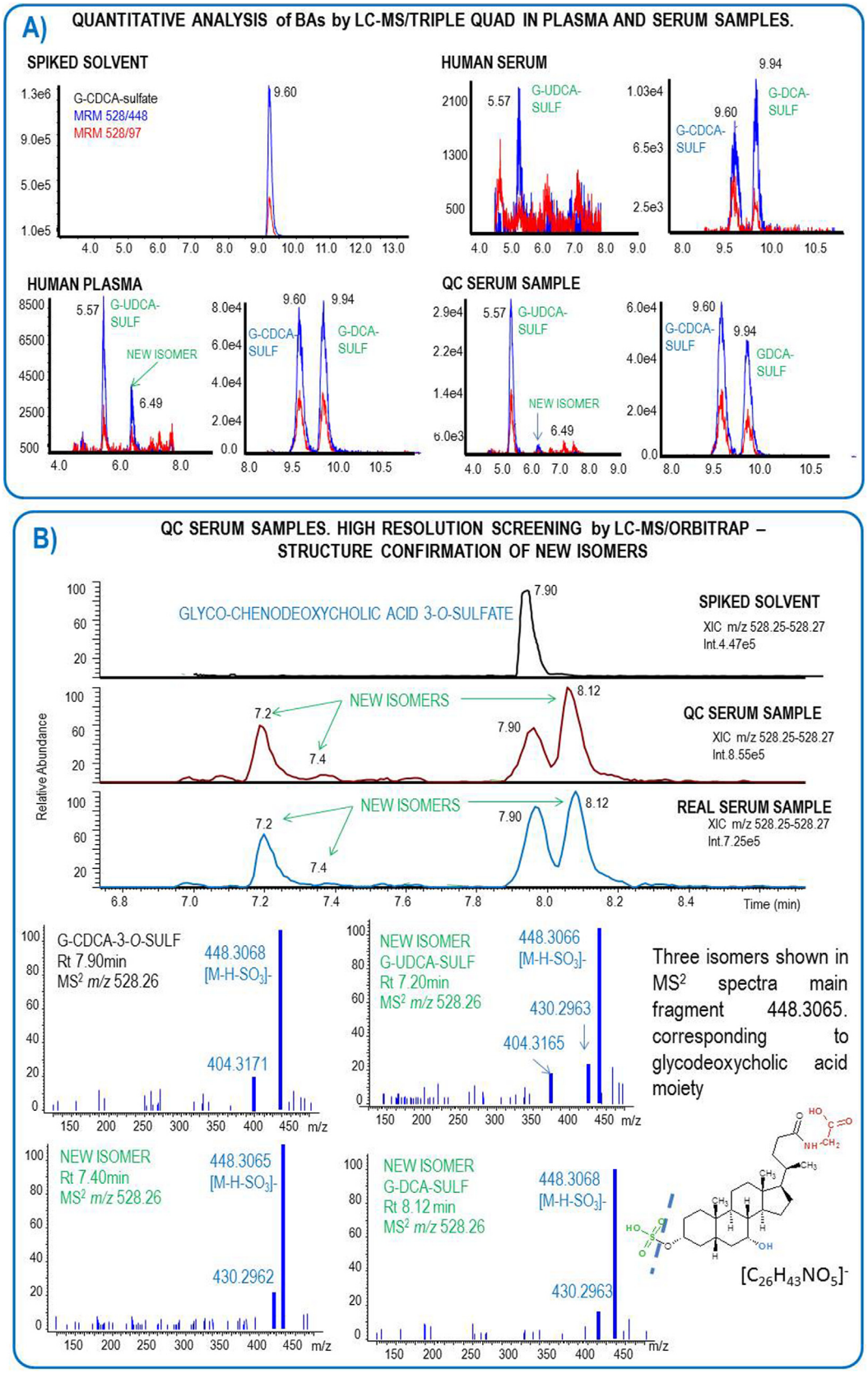

Fig. 2. Confirmation of the presence of additional BAs isomers: glycochenodeoxycholic acid sulfate isomers. Panel A: unscheduled screening with LC-Triple Quad mass spectrometer; Panel B: untargeted screening and MS/MS analysis with LC-HR Orbitrap mass spectrometer.

Table 2
LOD, LOQ, linearity range and matrix effect of bile acids in plasma and human serum.

	Bile Acids	Solvent	Human plasma	Human serum
	Lithocholic acid	y = 39.347x + 0.6252	y = 32.627x – 1.56	y = 36.873x – 0.1758
	Linearity range μM	0.018-2.25 μM	0.018-2.25 μM	0.018-2.25 μM
1	% Matrix effect	–	−20.6	−6.7
	LOD (μM)	LOD = 0.001	LOD =0.001	LOD =0.001
	LOQ (μM)	LOQ = 0.037	LOQ =0.0375	LOQ =0.0375
	6-ketolithocholic acid	y= 2.9399x + 0.0861	y = 2.8836x + 0.1051	y = 2.8967x + 0.0846
	Linearity range μM	0.002-2.25 μM	0.018-2.25 μM	0.018-2.25 μM
2	% Matrix effect	–	−2.0	−1.5
	LOD (μM)	LOD = 0.0020	LOD = 0.002	LOD = 0.002
	LOQ (μM)	LOQ= 0.006	LOQ = 0.007	LOQ = 0.006
	7-ketolithocholic acid	y= 0.3595x + 0.0011	y = 0.3478x + 0.0019	y = 0.3643x – 0.00120.998
	Linearity range μM	0.002-2.25 μM	0.018-2.25 μM	0.018-2.25 μM
3	% Matrix effect	–	−3.4	1.2
	LOD (μM)	LOD = 0.005	LOD = 0.009	LOD = 0.005
	LOQ (μM)	LOQ = 0.015	LOQ = 0.02	LOQ = 0.02
	12-ketolithocholic acid	y = 0.0406x + 0.0004 R^2 = 0.998	y = 0.0423x – 0.001	y = 0.0394x – 0.0002 R^2 = 0.996
	Linearity range μM	0.03-2.0 μM	0.075-2.25 μM	0.075-2.25 μM
4	% Matrix effect	–	−7.3	−4.6
	LOD (μM)	LOD = 0.015	LOD = 0.0375	LOD = 0.0375
	LOQ (μM)	LOQ = 0.05	LOQ = 0.20	LOQ = 0.20
	Murocholic acid	y = 3.0371x + 0.0219	y = 3.041x + 0.0369	y = 3.0274x + 0.0103
	Linearity range μM	0.002-2.25 μM	0.018-2.25 μM	0.018-2.25 μM
5	% Matrix effect	–	0.1	−0.3
	LOD (μM)	LOD = 0.005	LOD = 0.009	LOD = 0.0075
	LOQ (μM)	LOQ = 0.018	LOQ = 0.031	LOQ = 0.025
	Ursodeoxycholic acid	y = 2.3504x – 0.0099	y = 2.2589x + 0.0848	y = 2.3615x + 0.0564
	Linearity range μM	0.002-2.25 μM	0.075-2.5 μM	0.018-2.25 μM
6	% Matrix effect	–	−4.1	0.4
	LOD (μM)	LOD = 0.007	LOD = 0.018	LOD = 0.018
	LOQ (μM)	LOQ = 0.02	LOQ = 0.075	LOQ = 0.06
	Hyodeoxycholic acid	y = 4.9566x + 0.0278	y = 5.5892x + 0.0842	y = 5.5961x + 0.0809
	Linearity range μM	0.009-2.25 μM	0.018-2.25 μM	0.018-2.25 μM
7	% Matrix effect	–	11.3	11.4
	LOD (μM)	LOD = 0.006	LOD = 0.018	LOD = 0.014
	LOQ (μM)	LOQ = 0.02	LOQ = 0.0625	LOQ = 0.048
	Chenodeoxycholic acid	y = 2.5399x + 0.0022	y = 2.7833x + 0.3433	y = 2.8056x + 0.2651
	Linearity range μM	0.002-2.25 μM	0.11-2.25 μM	0.11-2.25 μM
8	% Matrix effect	–	8.7	9.5
	LOD (μM)	LOD = 0.003	LOD = 0.003	LOD =0.003
	LOQ (μM)	LOQ = 0.011	LOQ = 0.1125	LOQ = 0.1125
	Deoxycholic acid	y = 0.0433x – 0.0003	y = 0.0419x + 0.0019	y = 0.0443x + 0.0015
	Linearity range μM	0.005-2.25 μM	0.075-2.25 μM	0.075-2.25 μM
9	% Matrix effect	–	−3.3	1.6
	LOD (μM)	LOD = 0.005	LOD = 0.01	LOD = 0.01
	LOQ (μM)	LOQ = 0.018	LOQ = 0.075	LOQ = 0.075
	Dehydrocholic acid	y = 14.293x + 0.4356	y = 17.313x + 2.2913	y = 17.026x + 2.5153
	Linearity range μM	0.002-2.25 μM	0.1125-2.25 μM	0.1125-2.25 μM
10	% Matrix effect	–	17.4	16.0
	LOD (μM)	LOD = 0.003	LOD = 0.003	LOD =0.003
	LOQ (μM)	LOQ = 0.010	LOQ = 0.1125	LOQ = 0.1125
	7-dehydrocholic acid	y = 4.0265x + 0.0384	y = 3.8856x + 0.1439	y = 3.7806x + 0.1324
	Linearity range μM	0.075-2.25 μM	0.075-2.25 μM	0.075-2.25 μM
11	% Matrix effect	–	−3.6	−6.5
	LOD (μM)	LOD = 0.002	LOD = 0.005	LOD = 0.0023
	LOQ (μM)	LOQ = 0.007	LOQ = 0.075	LOQ = 0.075
	Ursocholic acid	y = 2.0485x + 0.0312	y = 2.2044x – 0.058	y = 2.0478x + 0.0412
	Linearity range μM	0.002-2.25 μM	0.018-2.25 μM	0.018-2.25 μM
12	% Matrix effect	–	7.1	−0.1
	LOD (μM)	LOD = 0.002	LOD = 0.005	LOD = 0.003
	LOQ (μM)	LOQ = 0.007	LOQ = 0.018	LOQ = 0.011
	Alfa-muricholic acid	y = 1.6162x + 0.0076	y = 1.7322x – 0.0431	y = 1.6272x + 0.0215
	Linearity range μM	0.002-2.25 μM	0.018-2.25 μM	0.018-2.25 μM
13	% Matrix effect	–	6.7	0.7
	LOD (μM)	LOD =0.0006	LOD = 0.008	LOD =0.004
	LOQ (μM)	LOQ =0.002	LOQ = 0.027	LOQ = 0.014
	Beta-muricholic acid	y = 2.2879x – 0.0321	y = 2.2974x – 0.0691	y = 2.1156x + 0.0394
	Linearity range μM	0.002-2.25 μM	0.018-2.25 μM	0.018-2.25 μM
14	% Matrix effect	–	0.4	−8.2
	LOD (μM)	LOD = 0.001	LOD = 0.005	LOD =0.009
	LOQ (μM)	LOQ = 0.004	LOQ = 0.018	LOQ =0.03

Table 2 (*Continued*)

	Bile Acids	Solvent	Human plasma	Human serum
	Hyocholic acid	y = 2.7024x – 0.013	y = 2.7871x – 0.0415	y = 2.6038x + 0.0857
	Linearity range μM	0.018-2.25 μM	0.018-2.25 μM	0.037-2.25 μM
15	% Matrix effect	–	3.0	−3.8
	LOD (μM)	LOD = 0.003	LOD =0.012	LOD =0.005
	LOQ (μM)	LOQ = 0.01	LOQ =0.04	LOQ =0.037
	Allocholic acid	y = 1.5086x – 0.0361	y = 1.5112x – 0.0352	y = 1.3472x + 0.0629
	Linearity range μM	0.010-2.25 μM	0.1125-2.25 μM	0.1125-2.25 μM
16	% Matrix effect	–	0.2	−12.0
	LOD (μM)	LOD =0.004	LOD = 0.007	LOD = 0.006
	LOQ (μM)	LOQ =0.015	LOQ = 0.1125	LOQ = 0.1125
	Cholic acid	y = 1.4762x + 0.1326	y = 1.6127x – 0.025	y = 1.481x + 0.2216
	Linearity range μM	0.005-6.25 μM	0.22-6.75 μM	0.05-6.25 μM
17	% Matrix effect	–	8.5	0.3
	LOD (μM)	LOD =0.001	LOD = 0.007	LOD = 0.007
	LOQ (μM)	LOQ =0.005	LOQ =0.22	LOQ =0.05
	Glycolithocholic acid	y = 0.4948x + 7E-05	y = 0.5017x + 0.005	y = 0.5293x + 0.0039
	Linearity range μM	0.002-2.25 μM	0.018-2.25 μM	0.018-2.25 μM
18	% Matrix effect	–	1.4	6.5
	LOD (μM)	LOD = 0.001	LOD = 0.0013	LOD = 0.0007
	LOQ (μM)	LOQ = 0.002	LOQ = 0.0043	LOQ = 0.0022
	Glycoursodeoxycholic acid	y = 2.9414x – 0.0043	y = 2.9493x + 0.2002	y = 3.0777x + 0.1272
	Linearity range μM	0.002-2.25 μM	0.11-2.25 μM	0.0357-2.25 μM
19	% Matrix effect	–	0.3	4.4
	LOD (μM)	LOD =0.002	LOD =0.003	LOD =0.002
	LOQ (μM)	LOQ =0.007	LOQ =0.11	LOQ =0.0357
	Glycohyodeoxycholic acid	y = 3.1314x – 0.0232	y = 3.0693x + 0.0314	y = 3.1113x + 0.0128
	Linearity range μM	0.002-2.25 μM	0.018-2.25 μM	0.018-2.25 μM
20	% Matrix effect	–	−2.0	−0.7
	LOD (μM)	LOD = 0.001	LOD = 0.005	LOD =0.003
	LOQ (μM)	LOQ = 0.005	LOQ = 0.017	LOQ =0.011
	Glycochenodeoxycholic acid	y = 2.9844x + 0.0345	y = 2.8614x + 1.2201	y = 3.0024x + 1.1857
	Linearity range μM	0.002-2.25 μM	0.1125-2.25 μM	0.1875-2.25 μM
21	% Matrix effect	–	−4.3	0.6
	LOD (μM)	LOD = 0.0009	LOD = 0.0025	LOD = 0.0025
	LOQ (μM)	LOQ = 0.003	LOQ = 0.1125	LOQ = 0.1875
	Glycodeoxycholic acid	y = 3.0412x + 0.0428	y = 3.0431x + 0.3275	y = 3.2388x + 0.36
	Linearity range μM	0.002-2.25 μM	0.075-2.25 μM	0.075-2.25 μM
22	% Matrix effect	–	0.1	6.1
	LOD (μM)	LOD = 0.002	LOD = 0.004	LOD = 0.003
	LOQ (μM)	LOQ = 0.007	LOQ =0.075	LOQ = 0.075
	Lithocholic acid-3-*O*- sulfate	y = 363.79x + 4.214	y = 336.94x – 16.18	y = 362.62x + 4.0233
	Linearity range μM	0.002-2.25 μM	0.018-2.25 μM	0.018-2.25 μM
23	% Matrix effect	–	−8.0	−0.3
	LOD (μM)	LOD =0.0007	LOD =0.0015	LOD =0.0015
	LOQ (μM)	LOQ =0.002	LOQ =0.005	LOQ =0.005
	Glycodehydrocholic acid	y = 2.8462x – 0.0673	y = 3.1175x + 0.0281	y = 3.2372x + 0.0023
	Linearity range μM	0.018-2.25 μM	0.018-2.25 μM	0.018-2.25 μM
24	% Matrix effect	–	8.7	12.1
	LOD (μM)	LOD =0.002	LOD =0.003	LOD =0.005
	LOQ (μM)	LOQ =0.005	LOQ =0.009	LOQ =0.007
	Glycohyocholic acid	y = 26.439x + 0.0676	y = 23.831x + 1.7702	y = 24.492x + 1.3018
	Linearity range μM	0.002-2.25 μM	0.018-2.25 μM	0.018-2.25 μM
25	% Matrix effect	–	−10.9	−8.0
	LOD (μM)	LOD =0.0012	LOD =0.003	LOD =0.003
	LOQ (μM)	LOQ = 0.004	LOQ = 0.018	LOQ = 0.018
	Glycocholic acid	y = 16.085x + 0.5715	y = 17.571x + 2.4586	y = 16.94x + 1.901
	Linearity range μM	0.06525-2.25 μM	0.225-2.25 μM	0.225-2.25 μM
26	% Matrix effect	–	8.5	5.0
	LOD (μM)	LOD = 0.002	LOD = 0.001	LOD = 0.001
	LOQ (μM)	LOQ = 0.004	LOQ =0.225	LOQ =0.225
	Taurolithocholic acid	y = 18.704x + 0.7332	y = 21.089x + 0.1923	y = 18.624x + 1.0972
	Linearity range μM	0.002-2.25 μM	0.075-2.25 μM	0.0375-2.25 μM
27	% Matrix effect	–	11.3	−0.5
	LOD (μM)	LOD = 0.001	LOD = 0.003	LOD =0.0025
	LOQ (μM)	LOQ = 0.004	LOQ =0.075	LOQ =0.0375
	Cholic acid -7-*O*-sulfate	y = 0.5247x + 0.0014	y = 0.4012x – 0.0089	y = 0.5798x – 0.0011
	Linearity range μM	0.002-2.25 μM	0.1875-2.25 μM	0.1875-2.25 μM
28	% Matrix effect	–	−30.7	9.3
	LOD (μM)	LOD =0.0079	LOD =0.005	LOD =0.005
	LOQ (μM)	LOQ =0.0026	LOQ =0.1855	LOQ =0.18755
	Tauroursodeoxycholic acid	y = 3.879x + 0.0012	y = 3.6865x + 0.1048	y = 3.8371x + 0.0874
	Linearity range μM	0.002-2.25 μM	0.018-2.25 μM	0.018-2.25 μM
29	% Matrix effect	–	−5.2	−1.1
	LOD (μM)	LOD=0.0009	LOD = 0.003	LOD =0.0018
	LOQ (μM)	LOQ=0.003	LOQ = 0.008	LOQ =0.006

Table 2 (*Continued*)

	Bile Acids	Solvent	Human plasma	Human serum
	Taurohyodeoxycholic acid	y = 7.3134x – 0.0059	y = 8.2186x + 0.0279	y = 6.2177x + 0.3263
	Linearity range μM	0.002-2.25 μM	0.075-2.25 μM	0.018-2.25 μM
30	% Matrix effect	–	11.0	−17.6
	LOD (μM)	LOD = 0.0005	LOD = 0.006	LOD = 0.003
	LOQ (μM)	LOQ = 0.002	LOQ = 0.075	LOQ = 0.018
	Taurochenodeoxycholic acid	y = 13.748x + 0.1891	y = 15.611x + 0.7366	y = 13.061x + 1.201
	Linearity range μM	0.002-2.25 μM	0.075-1.5 μM	0.018-2.25 μM
31	% Matrix effect	–	11.93	−5.3
	LOD (μM)	LOD = 0.002	LOD = 0.003	LOD = 0.004
	LOQ (μM)	LOQ = 0.006	LOQ = 0.075	LOQ = 0.018
	Taurodeoxycholic acid	y = 4.5736x + 0.1717	y = 4.4449x + 0.0885	y = 3.8011x + 0.2929
	Linearity range μM	0.002-2.25 μM	0.075-2.25 μM	0.0375-2.25 μM
32	% Matrix effect	–	−2.9	−20.3
	LOD (μM)	LOD = 0.002	LOD = 0.003	LOD = 0.003
	LOQ (μM)	LOQ = 0.006	LOQ = 0.075	LOQ = 0.0375
	Tauro Omega-muricholic acid	y = 6.5867x + 0.0131	y = 6.62x + 0.0474	y = 6.6465x + 0.0389
	Linearity range μM	0.002-2.25 μM	0.018-2.25 μM	0.018-2.25 μM
33	% Matrix effect	–	0.5	0.9
	LOD (μM)	LOD=0.002	LOD = 0.008	LOD = 0.04
	LOQ (μM)	LOQ=0.005	LOQ = 0.018	LOQ = 0.14
	Tauro Alfa-muricholic acid	y = 11.588x + 0.0266	y = 11.475x + 0.1612	y = 11.417x + 0.1037
	Linearity range μM	0.002-2.25 μM	0.018-2.25 μM	0.018-2.25 μM
34	% Matrix effect	–	−1.0	−1.6
	LOD (μM)	LOD = 0.002	LOD = 0.003	LOD =0.002
	LOQ (μM)	LOQ = 0.003	LOQ = 0.009	LOQ =0.003
	Tauro Beta-muricholic acid	y = 26.513x + 0.9878	y = 32.7x – 0.8217	y = 26.85x + 1.2605
	Linearity range μM	0.002-2.25 μM	0.018-2.25 μM	0.018-2.25 μM
35	% Matrix effect	–	18.9	1.3
	LOD (μM)	LOD = 0.0009	LOD = 0.002	LOD = 0.001
	LOQ (μM)	LOQ = 0.0031	LOQ = 0.008	LOQ = 0.003
	Taurohyocholic acid	y = 42.941x + 1.4565	y = 46.906x + 0.925	y = 38.799x + 2.0544
	Linearity range μM	0.018-2.25 μM	0.018-2.25 μM	0.018-2.25 μM
36	% Matrix effect	–	8.5	−10.7
	LOD (μM)	LOD = 0.0005	LOD =0.0008	LOD =0.0009
	LOQ (μM)	LOQ = 0.002	LOQ =0.003	LOQ =0.015
	Taurocholic acid	y = 15.629x + 1.7129	y = 18.769x + 0.4265	y = 18.855x + 0.1768
	Linearity range μM	0.006-4.5 μM	0.05625-2.25 μM	0.05625-2.25 μM
37	% Matrix effect	–	16.7	17.1
	LOD (μM)	LOD = 0.0006	LOD =0.0008	LOD =0.0008
	LOQ (μM)	LOQ = 0.007	LOQ = 0.05625	LOQ = 0.05625
	Glycochenodeoxycholic acid-3-*O*- sulfate	y = 2.3708x + 0.0088	y = 2.7062x + 0.0622	y = 2.4321x + 0.0643
	Linearity range μM	0.00918-1.1025 μM	0.055-1.10 μM	0.01837-1.10 μM
38	% Matrix effect	–	12.4	2.5
	LOD (μM)	LOD = 0.0005	LOD = 0.001	LOD = 0.001
	LOQ (μM)	LOQ = 0.002	LOQ = 0.05	LOQ = 0.018
	Taurolithocholic sulfate	y = 2.5939x-0.1969 R^2 = 0.993	y =6.898x+0.5669 R^2 =0.997	y =2.065x-0.008 R^2 =0.991
	Linearity range μM	0.02-2.25 μM	0.0375-2.25 μM	0.0375-2.25 μM
39	% Matrix effect	–	63.2	25.3
	LOD (μM)	LOD =0.008	LOD =0.05	LOD = 0.01875
	LOQ (μM)	LOQ = 0.03	LOQ =0.2	LOQ =0.05
	Chenodeoxycholic acid -3-β-glucuronide	y = 0.3665x + 0.007	y = 0.4075x + 0.0016	y = 0.417x + 0.0036
	Linearity range μM	0.002-2.25 μM	0.018-2.25 μM	0.018-2.25 μM
40	% Matrix effect	–	10.1	12.1
	LOD (μM)	LOD = 0.002	LOD = 0.003	LOD = 0.008
	LOQ (μM)	LOQ = 0.006	LOQ = 0.01	LOQ = 0.026
	Taurocholic-3-*O*-sulfate	y =2.9741x-0.2027 R^2 =0.0998	y=4.9111+0.1333 R^2 =0.993	y=2.0221x-0.0255 R^2 =0.997
	Linearity range μM	0.01875-2.25	0.0375-0.75	0.075-2.25
41	% Matrix effect	–	39	−1.48
	LOD (μM)	LOD = 0.005	LOD =0.05	LOD =0.0375
	LOQ (μM)	LOQ = 0.02	LOQ =0.20	LOQ =0.075

4.3. Linearity in solvent and matrices, matrix effect

Two types of matrices: human plasma and human serum from Sigma Aldrich and solvent (methanol/ water ratio 1:1) were used for evaluation of matrix effect. Each matrix type and solvent were spiked with mix of native BAs ranging from 0.0005 μM to 5 μM. The IS concentrations were kept constant at all the calibration points (0.2 μM) and were added before extraction procedure, while external standard was added after extraction (during re-dissolving step). Calibration curves were constructed using ratio between quantifier MRM of native compound vs quantifier MRM of labelled bile acid. Supplementary Table 2 reports all native bile acids and corresponding labelled bile acid used for quantification. Whenever possible, bile acids were quantified using ratio with its corresponding deuterated standards. For other BAs the nearest eluting labelled isomer was used, such as UDCA-d4 for quantification of MuroCA and HDCA, or G-UDCA-d4 for quantification of G-HDCA. For KLCA isomers cholic acid d4 was used, while for CDCA-GLC isomers - the CDCA-d4 was used, in both cases to account for recovery loss. Such strategy was successfully applied in several investigations [15,16,29]. See Supplementary Table 2 for more details. Determination coefficients (R^2) greater than 0.99 were obtained for all

compounds using weighted (1/x2) linear calibration curves. Linearity ranges in μM are given in Table 2.

Among the studied compounds, thirty nine out of forty-one presented matrix effects within ± 20%, and only two compounds showed absolute matrix effects higher than 20% namely cholic acid sulfate in plasma - 30%, and taurolithocholic acid sulfate in plasma 63% and in serum 25%. In those three cases results require adjustment for matrix effect during quantification. Calibration curves in solvent were chosen for quantitative determinations as an appropriate calibration technique as matrix effect was negligible for most of bile acids (< 10%), and acceptable for the rest (< 20%) – See Table 2 for details.

4.4. Selectivity, LOD, LOQ, recovery

The selectivity of the method was assessed via the analysis of procedural blank samples. MRM chromatograms obtained for quantifier and qualifier MS/MS transitions were checked for co-eluting interferences at the retention times of the corresponding BAs. No interferences were observed at the retention times of analytes ±0.1 min in any of the transitions.

The LODs in solvent ranged between 0.0002 μM – 0.03 μM, in human plasma from 0.0003 μM – 0.0375 μM; while in human serum from 0.008 μM - 0.04 μM. The LOQ varied between 0.0007 μM - 0.1125 μM; 0.003 μM - 0.225 μM and 0.002 μM - 0.225 μM; respectively for solvent, human plasma, and human serum. Details regarding regression curves, LOD, LOQ, and matrix effects for all compounds can be found in Table 2. In order to assess the efficiency of extraction, two experiments were performed to verify recoveries. In first experiment serum samples were spiked with a pool of labelled with deuterium standards at levels 0.25 μM; 0.5 μM and 1 μM. For recovery assessment samples was prepared in triplicate, while spiking was done before and after extraction for further comparison of peak areas. For all compounds satisfactory recoveries were found between 73% and 105%, details are given in Supplement Table 4. Second experiment included recovery assessment for native bile acids. Serum and plasma samples from Sigma Aldrich were first analysed to quantify bile acid content, and further on spiked with native bile acids at two levels corresponding to 150% and 250% of the original content. Recoveries in serum for spiking level 150% varied from 78% to 113%, while for spiking level of 250% varied between 75% and 113%. Similar satisfactory results were obtained for plasma, with recovery in range 80%–113% and 75–112% for spiking levels 150% and 250% respectively. Detailed information are shown in Supplementary Table 5. Additionally recovery calculated for each study sample and QC samples are given in Supplementary Table 6.

4.5. Determination and quantification of bile acids in serum after berries ingestion

The method was used to analyze BAs in human serum samples that were collected from 20 volounteers within six hours after consumption of berries. Ten participants consumed *Vaccinium corymbosum*, while in parallel other ten consumed *Vaccinium myrtillus*. Among forty nine BAs included in the method, thirty four were quantified in serum: nine taurine- conjugated, seven glycine- conjugated, and nine unconjugated. For the first time four sulfate and five glucuronide bile acids were quantified in a postprandial kinetic study (See Table 3 for details). Sulfate conjugates that occurred at the highest concentration were G-CDCA-3*O*- sulfate 34.5 nM (± 0.24 SE), followed by G-DCA sulfate 22.7 nM (±0.14 SE) and G-UDCA sulfate 12.4 nM (± 0.09 SE). Five glucuronide conjugates of dihydroxy BAs isomers were found at following concentrations: 36.2 nM ± 0.63 (Isomer at Rt 9.16 min); 33.2 nM ± 0.22 (Isomer at Rt 12.97 min); 18.8 μM ± 0.13 (Isomer at Rt 9.60 min); 11.2 nM ± 0.05 (Isomer at Rt 13.5 min); 9.7 nM ± 0.04 (Isomer at Rt 13.20 min). Data resuming range of concentrations found for each compound is given in Table 3. Values are expressed as mean ± SE of concentration given in nanoMolar. Considering high variability of concentrations found in samples, Table 3 contains also information regarding number of samples below LOD and below LOQ. It is well know that BAs occur in biological fluids at concentrations that vary even up to five orders of magnitude, and we found some difficulties in quantification of BAs present in low concentrations. Bile acids found below LOD and/or LOQ were dehydroCA, G-dehydroCA, AlloCA, β-MCA, UrsoCA, T-HDCA, T-β-MCA, HDCA, MuroCA, TCA-3*O*-SULF, CA-7*O*-SULF, 6-KLCA and 12-KLCA, see Table 3 for more details. These BAs they were excluded from statistical analysis. The range of concentrations found in our study is in a good agreement with previous reports in the in literature, with glycine-conjugated BAs being found at higher concentration than taurine-conjugated and free BAs [19,20]. The PCA score plot did not show any evident batch effect or outlier sample while QC samples clustered tightly together (Supplementary Material Fig. 1).

Fasting plasma BA levels presented a large inter-individual variation in both concentrations and composition (Fig. 3 Panel A), with a 11-fold variation for the sum of all BA. The most abundant BA species were the free and glycine-conjugated forms. In fasting state, free BA represented $\tilde{4}1\%$ (range: 3–81%) and glycine-conjugated $\tilde{4}0\%$ (range: 11–74%) of total BA, whereas glycine-sulfate-conjugated, taurine-conjugated, sulfates- and glucuronides-conjugated and others accounted for $\tilde{4}\%$ (range: 1–12%), $\tilde{6}\%$ (range: 1–24%), $\tilde{6}\%$ (range: 1–25%) and $\tilde{3}\%$ (range: 1–5%), respectively. Interestingly, these findings are in good agreement wih recent results by Fiamoncini et al 2018 [4].

The postprandial response measured by AUCs also revealed a high inter-individual variability across the volunteers (16-fold, Fig. 3 Panel B). Total BA concentrations in fasting conditions correlated significantly with postprandial response measured by AUC values was observed [$r = 0.72$; $p < 0.001$]. Bile acids contributing the most to total sum were always free BA and glycine-conjugated BAs, what is in a good agreement with Han et al. 2015 (Fig. 3, Panel B). Modifications in the proportion of circulating BA were also observed during this period. Levels of free BA dropped from $\tilde{4}1\%$ in fasting conditions to $\tilde{2}5$-35% during the postprandial state, whereas glycine-conjugated BA went from $\tilde{4}0\%$ to $\tilde{5}0\%$. The kinetic curves corresponding to the different classes of BA revealed differences in their behavior (Fig. 3, Panel C). Both glycine- and taurine-conjugated BA showed a clear increase in their plasmatic levels immediately after the food intake, reaching their maximum levels after 1h. On the other hand, although also free BA reached their maximum levels after 1h, they showed an initial decrease during the first 30 min.

No statistical differences were found between two types of berries ingestion during post-prandial responses (p-values 0.262−0.812). Although fasting and postprandial BAs concentrations revealed high inter-individual variability, both supplements showed similar postprandial kinetics, with maximum concentration of total sum of BAs occurring between 1 h and 2 h postprandial (See Fig. 4, Panel A).

Statistically significant differences were found in postprandial response of glycine-sulfate BAs concentrations between males and females (p-value = 0.040), while for classes Free BAs, Total BAs and Glucuronide and sulfates BAs p-values were just above cut-off limit 0.05, suggesting that gender differences have a strong impact on overall bile acid homeostasis. Panel B in Fig. 3 shows postprandial kinetic curves for total sum of BAs, sum of Free BAs, sum of Glycine-Sulfates BAs, sum of Sulfates BAs and Glucuronide BAs and sum of Others BAs, with found in higher concentrations in males. This observation was also apparent in the PCA biplot (Panel B of Fig. 4). The Tmax of total sum BAs as well as for Free BAs class for

Table 3
Resume of quantification for bile acids in serum samples from *Vaccinium corymbosum* and *Vaccinium myrtillus* consumption. Concentration expressed as nanoMolar: mean ± standard error.

Free BAs	CA	CDCA	DCA	UDCA	LCA	HCA	MuroCA*	AlloCA*	β-MCA*	UrsoCA*	HDCA*
Mean ± SE (nM)	226.5 ± 5.6	312.1 ± 6.3	295.9 ± 2.6	110.6 ± 0.99	63.8 ± 0.3	29.0 ± 0.24	–	–	–	–	–
Min (nM)	12.5	11.8	12.5	20.5	27.6	7.6	–	–	–	–	–
Max (nM)	3704.9	4565.9	1707.0	575.4	121.1	132.5	–	–	–	–	–
<LOD	0	0	0	24	25	18	108	108	108	108	108
<LOQ	1	3	0	12	63	36	–	–	–	–	–

Taurine-BAs	T-UDCA	T-CDCA	T-DCA	T-Alfa MCA	T- Omega MCA	T-HCA	T-LCA-SULF	T-CA	T-LCA	T-HDCA*	T-Beta MCA*
Mean ± SE (nM)	8.8 ± 0.63	81.9 ± 1.23	59.0 ± 1.57	11.0 ± 0.05	22.7 ± 0.1	2.1 ± 0.006	31.6 ± 0.11	119.3 ± 2.81	8.0 ± 0.06	–	–
Min (nM)	3.2	6.1	2.4	4.7	10.0	1.7	19.3	7.4	4.2	–	–
Max (nM)	30.1	1118.6	1500.8	25.8	52.8	3.6	68.5	1956.0	38.0	–	–
<LOD	33	0	0	27	44	80	43	11	0	52	107
<LOQ	37	0	8	38	34	15	28	41	71	56	1

Glyco-BAs	G-LCA	G-CA	G-HCA	G-UDCA	G-CDCA	G-DCA	G-HDCA	G-dehydroCA*
Mean ± SE (nM)	19.4 ± 0.14	263.5 ± 4.22	8.4 ± 0.07	71.5 ± 0.7	610.4 ± 4.9	250.1 ± 3.9	8.0 ± 0.02	–
Min (nM)	4.2	15.7	3.5	5.7	41.4	9.2	6.3	–
Max (nM)	80.9	3510.8	50.1	386.3	3323.1	3621.0	10.8	–
<LOD	0	0	6	0	0	0	63	108
<LOQ	3	0	30	2	0	0	32	–

Glycine-sulfates BAs	G-CDCA-3-*O*-sulfate	G-UDCA-sulfate	G-DCA-sulfate	G-CDCA-sulfate Isomer (Rt 6.49 min)*
Mean ± SE (nM)	34.5 ± 0.25	12.4 ± 0.09	22.7 ± 0.14	–
Min (nM)	12.5	12.5	12.5	–
Max (nM)	155.8	46.0	64.1	–
<LOD)	0	0	0	–
<LOQ	0	0	0	108

Sulfates BAs and Glucuronides BAs	CDCA-glucuronide	DihydroxyBA-GLC (Is.1) (Rt 9.16 min)	DihydroxyBA-GLC (Is.3) (Rt 13.20min)	DihydroxyBA-GLC (Is.2) (Rt 9.60 min)	DihydroxyBA-GLC (Is.4) (Rt 13.57 min)	LCA-SULF	CA-SULF*	T-CA SULF*
Mean ± SE (nM)	33.2 ± 0.22	36.2 ± 0.63	9.7 ± 0.04	18.8 ± 0.13	11.2 ± 0.05	8.0 ± 0.1	–	–
Min (nM)	5.7	12.5	5.4	12.5	5.4	2.3	–	–
Max (nM)	98.5	479.8	20.5	87.2	25.3	54.7	–	–
<LOD	1	0	29	0	34	4	108	108
<LOQ	6	0	25	0	42	44	–	–

Others BAs	7-KLC	KLC-isomer (Rt 17.43 min)	7-dehydroCA	6-KLC*	12-KLC*	Dehydro-CA*	KLC-isomer (Rt 16.04 min)*
Mean ± SE (nM)	19.2 ± 0.1	78.3 ± 0.76	13.3 ± 0.04	–	–	–	–
Min (nM)	9.4	13.0	6.3	–	–	–	–
Max (nM)	54.4	503.5	19.7	–	–	–	–
<LOD	38	0	76	108	96	108	–
<LOQ	30	0	15	–	7	–	108

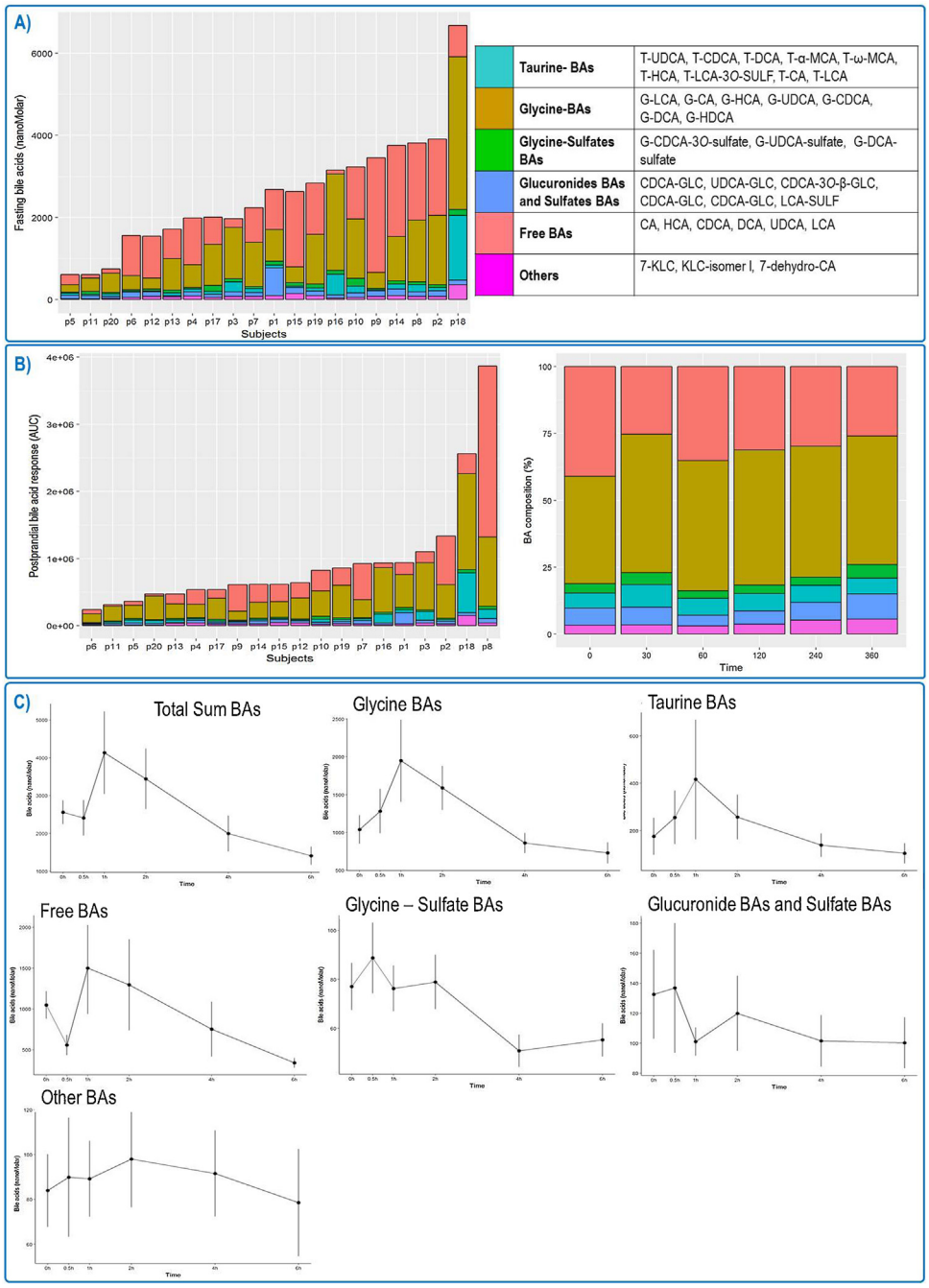

Fig. 3. Panel A: Fasting serum bile acid composition at subject/individual level (left). The table shows individual bile acids contributing to each BA class (right). Panel B: Postprandial bile acids response expressed as AUC curves for each subject (left), and contribution of each bile acid class at each time point expressed in % (right). Panel C: Kinetic curves of each bile acid class during 6 h postprandial. Bile acids concentration expressed in nanoMolar.

man was at 1 h postprandial, while in female at 2 h postprandial. These differences in Tmax between male and female are also in good agreement with recent study by Fiamoncini et al [4], which showed that women rich maximal BAs values after 60 min postprandial, while men in 30 min. However Fiamoncini showed that in woman BAs levels seemd higher than in man after OGT and MMT tests, what is exactly oposite to our results. The difference between our results and the one found in Fiamoncini is probably due to composition of ingested products: 75 g of glucose in water (OGTT) and high-fat, high-glucose, high-caloric drink (MMT), while berries supplement consised of very low sugar content (ca 4 mg/100 g [30]). Differences between BAs concentrations in males and females were also reported by Galman et al [31] showing that bile acid synthesis is almost 29% higher in men than in women. Trottier [22] found gender-related difference in the responses of various bile acids to fenofibrate intake, where bile acid concentration was significantly reduced only in men. Finally, a cluster analysis was performed to evaluate the potential existence of different patterns in postprandial BA response (Panel B of Fig. 5). Three clusters of subjects were identified and their differences in BA response were further examined in terms of individual BA responses. In most of cases, results suggest that the third cluster responded with the higher postprandial BA increases, with the exeption of sulfate and glucuronide conjugated BAs.

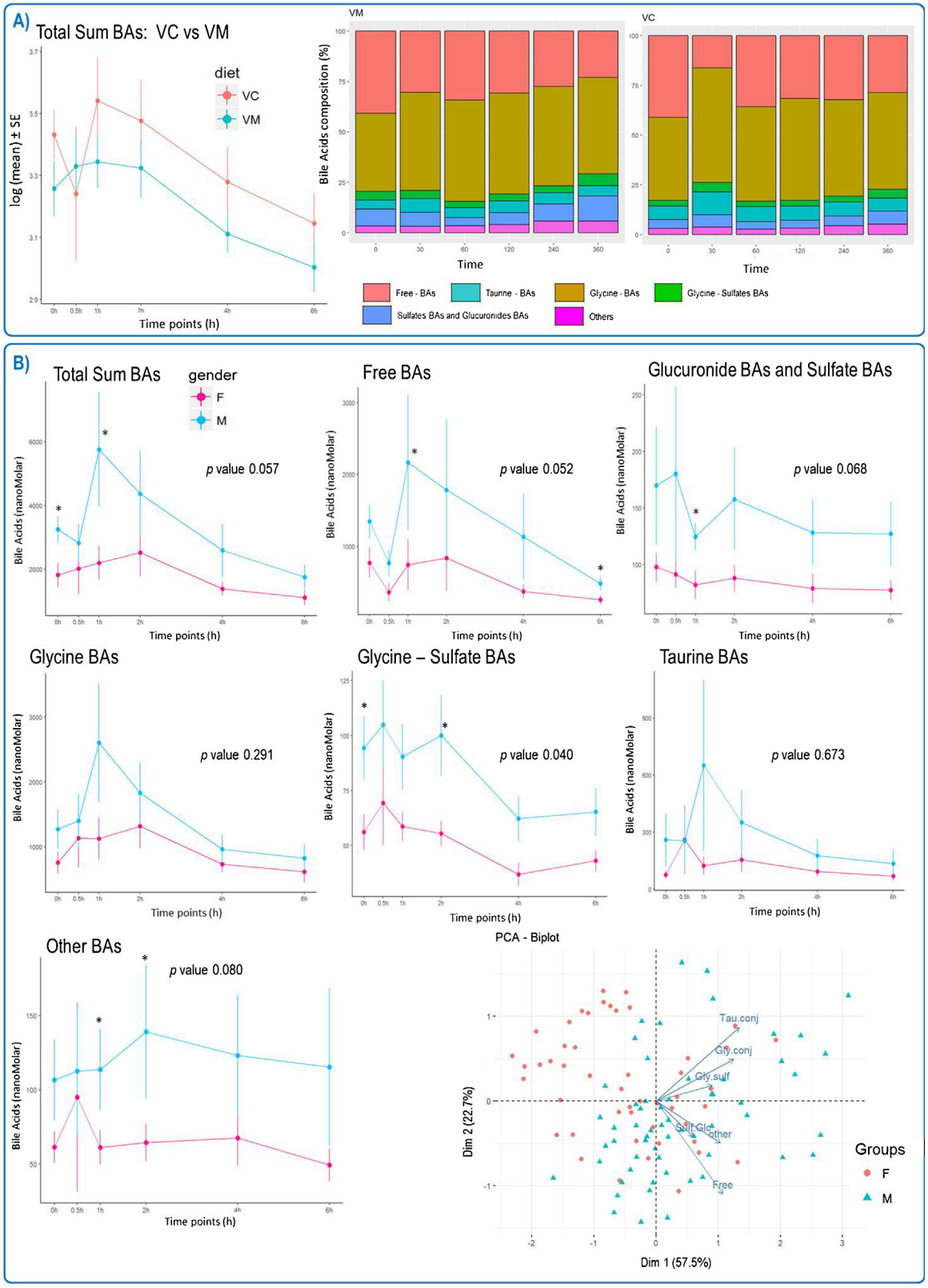

Fig. 4. Panel A: Kinetic curves of total bile acid excretion during 6 h postprandial for *Vaccinium corymbosum* (VC) and *Vaccinium myrtillus* (VM) intake (left). The percent stacked barcharts showing contribution of bile acid groups to total bile acids (in %) for two dietary interventions *Vaccinium corymbosum* (VC) and *Vaccinium myrtillus* (VM). Panel B: Kinetic curves for bile acids classes ploted for males and females with corresponsing *p* values resulting from comparison of AUC curves. Bile acids classes expressed in nanoMolar concentration, time points resulting statistically significant with *p*-value <0.05 are marked with asterix (*). The PCA Biplot (bottom right) shows scores coloured accroding to volunteers gender and loadings suggesting higher concentration of biles acids in males.

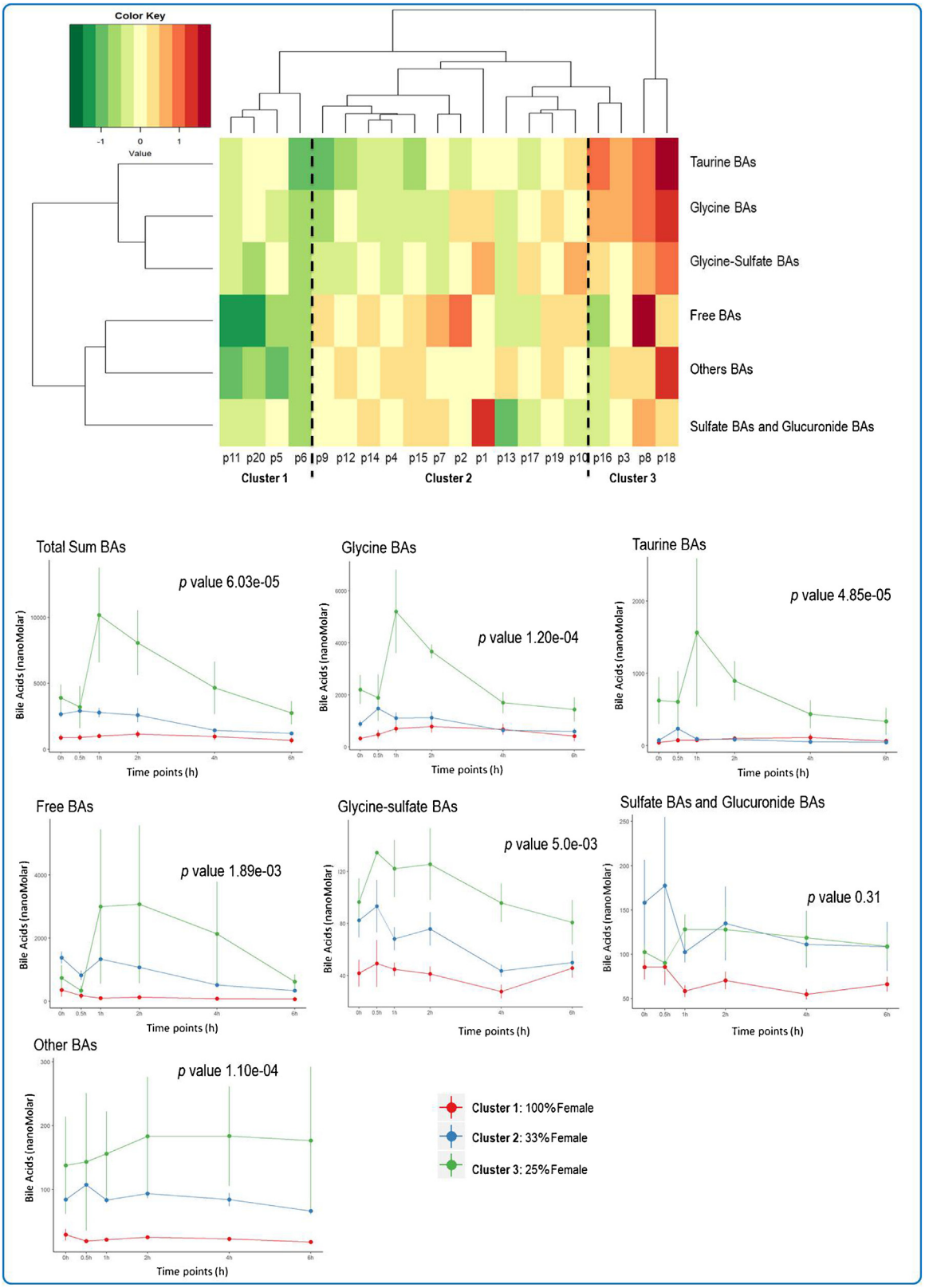

Fig. 5. Clustering of volunteers according to postprandial plasma bile acid kinetics. Heatmap shows clustering of volunteers based on plasma concentration profiles of bile acids. Postprandial kinetics for different bile acids classes for each of 3 clusters are accompanied by *p* value from comparison of area under the curve AUC.

5. Conclusions

An improved UHPLC-Triple Quad MS method was applied to study bile acids levels in serum samples from a kinetic study over 6 h postprandial after consumption of two types of berries. For the first time sulfates conjugated forms of bile acids were measured and quantified using deuterated bile acids internal standards. With this method it was possible to separate forty nine bile acids and quan-

tify them at trace nM levels. A strategy of scheduled/ unscheduled injections of real samples allowed us to find additional bile acid isomers not *a priori* included in the method, while high resolution full scan and MS/MS fragmentation analysis confirmed their structural adherence to the bile acid family. The applicability of the proposed method was assessed by analysing serum samples from a nutrikinetic challenge study with two different types of berries, which showed high inter-individual differences both in the concentrations and composition of plasmatic BAs in fasting and postprandial state. We found differences in bile acids quantity and time reaching maximal BAs concentrations between males and females, suggesting higher BA concentrations in males. Despite high inter-individual variability in fasting and postprandial states, we found three possible subgroups thorough hierarchical clustering. Values regarding the variability among all study volunteers and proportional distribution of BAs were in agreement with previous data measured in independent populations. These findings open new perspectives in understanding the role of the diet, and give an important impact on understanding of bile acid homeostasis and on future personalized nutrition strategies.

Funding

This work was supported by the Project "Cabala_diet&health" (http://www.cabalaproject.eu/) and received funding from the European Union's Horizon2020 research and innovation grant agreement No 696295 – ERA-Net Cofund ERA-HDHL "Biomarkers for Nutrition and Health implementing the JPI HDHL objectives" (https://www.healthydietforhealthylife.eu/). Additionally work was supported from the Autonomous Province of Trento, ADP 2018.

Declarations of interest

None.

Appendix A. Supplementary data

Supplementary material related to this article can be found, in the online version, at doi:https://doi.org/10.1016/j.jpba.2019.05.002.

References

[1] S.L. Long, C.G.M. Gahan, S.A. Joyce, Interactions between gut bacteria and bile in health and disease, Mol. Aspects Med. 56 (2017) 54–65, http://dx.doi.org/10.1016/j.mam.2017.06.002.
[2] A.F. Hofmann, L.R. Hagey, Bile acids: chemistry, pathochemistry, biology, pathobiology, and therapeutics, Cell. Mol. Life Sci. 65 (2008) 2461–2483, http://dx.doi.org/10.1007/s00018-008-7568-6.
[3] A.F. Hofmann, L.R. Hagey, Key discoveries in bile acid chemistry and biology and their clinical applications: history of the last eight decades, J. Lipid Res. 55 (2014) 1553–1595, http://dx.doi.org/10.1194/jlr.R049437.
[4] J. Fiamoncini, A.M. Yiorkas, K. Gedrich, M. Rundle, S.I. Alsters, G. Roeselers, T.J. van den Broek, T. Clavel, I. Lagkouvardos, S. Wopereis, G.S. Frost, B. van Ommen, A.I.F. Blakemore, H. Daniel, Determinants of post-prandial plasma bile acid kinetics in human volunteers, Am. J. Physiol. Gastrointest. Liver Physiol. (2017), http://dx.doi.org/10.1152/ajpgi.00157.2017, ajpgi.00157.2017.
[5] Y. Alnouti, Bile acid sulfation: a pathway of bile acid elimination and detoxification, Toxicol. Sci. 108 (2009) 225–246, http://dx.doi.org/10.1093/toxsci/kfn268.
[6] S.P.R. Bathena, S. Mukherjee, M. Olivera, Y. Alnouti, The profile of bile acids and their sulfate metabolites in human urine and serum, J. Chromatogr. B Anal. Technol. Biomed. Life Sci. 942–943 (2013) 53–62, http://dx.doi.org/10.1016/j.jchromb.2013.10.019.
[7] J.M. Ridlon, D.-J. Kang, P.B. Hylemon, Bile salt biotransformations by human intestinal bacteria, J. Lipid Res. 47 (2006) 241–259, http://dx.doi.org/10.1194/jlr.R500013-JLR200.
[8] S.I. Sayin, A. Wahlström, J. Felin, S. Jäntti, H.U. Marschall, K. Bamberg, B. Angelin, T. Hyötyläinen, M. Orešič, F. Bäckhed, Gut microbiota regulates bile acid metabolism by reducing the levels of tauro-beta-muricholic acid, a naturally occurring FXR antagonist, Cell Metab. 17 (2013) 225–235, http://dx.doi.org/10.1016/j.cmet.2013.01.003.
[9] S.A. Joyce, J. MacSharry, P.G. Casey, M. Kinsella, E.F. Murphy, F. Shanahan, C. Hill, C.G.M. Gahan, Regulation of host weight gain and lipid metabolism by bacterial bile acid modification in the gut, Proc. Natl. Acad. Sci. 111 (2014) 7421–7426, http://dx.doi.org/10.1073/pnas.1323599111.
[10] R. Zhu, Y. Hou, Y. Sun, T. Li, J. Fan, G. Chen, J. Wei, Pectin penta-oligogalacturonide suppresses intestinal bile acids absorption and downregulates the FXR-FGF15 Axis in high-cholesterol fed mice, Lipids 52 (2017) 489–498, http://dx.doi.org/10.1007/s11745-017-4258-x.
[11] B. Fotschki, J. Juśkiewicz, A. Jurgoński, N. Rigby, M. Sójka, K. Kołodziejczyk, A. Mackie, Z. Zduńczyk, Raspberry pomace alters cecal microbial activity and reduces secondary bile acids in rats fed a high-fat diet, J. Nutr. Biochem. 46 (2017) 13–20, http://dx.doi.org/10.1016/j.jnutbio.2017.03.004.
[12] B. Drzikova, G. Dongowski, E. Gebhardt, Dietary fibre-rich oat-based products affect serum lipids, microbiota, formation of short-chain fatty acids and steroids in rats, Br. J. Nutr. 94 (2005) 1012, http://dx.doi.org/10.1079/BJN20051577.
[13] L. Rizzetto, F. Fava, K.M. Tuohy, C. Selmi, Connecting the immune system, systemic chronic inflammation and the gut microbiome: the role of sex, J. Autoimmun. 92 (2018) 12–34, http://dx.doi.org/10.1016/j.jaut.2018.05.008.
[14] S.A. Joyce, C.G.M. Gahan, Bile acid modifications at the microbe-host interface: potential for nutraceutical and pharmaceutical interventions in host health, Annu. Rev. Food Sci. Technol. 7 (2016) 313–333, http://dx.doi.org/10.1146/annurev-food-041715-033159.
[15] L. Humbert, M.A. Maubert, C. Wolf, H. Duboc, M. Mahé, D. Farabos, P. Seksik, J.M. Mallet, G. Trugnan, J. Masliah, D. Rainteau, Bile acid profiling in human biological samples: comparison of extraction procedures and application to normal and cholestatic patients, J. Chromatogr. B Anal. Technol. Biomed. Life Sci. 899 (2012) 135–145, http://dx.doi.org/10.1016/j.jchromb.2012.05.015.
[16] J. Han, Y. Liu, R. Wang, J. Yang, V. Ling, C.H. Borchers, Metabolic profiling of bile acids in human and mouse blood by LC-MS/MS in combination with phospholipid-depletion solid-phase extraction, Anal. Chem. 87 (2015) 1127–1136, http://dx.doi.org/10.1021/ac503816u.
[17] W.J. Griffiths, J. Sjovall, Bile acids: analysis in biological fluids and tissues, J. Lipid Res. 51 (2010) 23–41, http://dx.doi.org/10.1194/jlr.R001941-JLR200.
[18] J. Han, Y. Liu, R. Wang, J. Yang, V. Ling, C.H. Borchers, Metabolic Profiling of Bile Acids in Human and Mouse Blood by LC-MS / MS in Combination with Phospholipid-Depletion Solid-Phase Extraction Metabolic Profiling of Bile Acids in Human and Mouse Blood by LC-MS/MS in Combination with Phospholipid-Depletion, 2014, pp. 1–20, http://dx.doi.org/10.1021/ac503816u.
[19] J. Huang, S. Praneeth, R. Bathena, I.L. Csanaky, Y. Alnouti, Simultaneous characterization of bile acids and their sulfate metabolites in mouse liver, plasma, bile, and urine using LC–MS/MS, J. Pharm. Biomed. Anal. 55 (2011) 1111–1119, http://dx.doi.org/10.1016/j.jpba.2011.03.035.
[20] M. Scherer, C. Gnewuch, G. Schmitz, G. Liebisch, Rapid quantification of bile acids and their conjugates in serum by liquid chromatography-tandem mass spectrometry, J. Chromatogr. B Anal. Technol. Biomed. Life Sci. 877 (2009) 3920–3925, http://dx.doi.org/10.1016/j.jchromb.2009.09.038.
[21] X. Cai, Y. Liu, X. Zhou, U. Navaneethan, B. Shen, B. Guo, An LC-ESI-MS method for the quantitative analysis of bile acids composition in fecal materials, Biomed. Chromatogr. 26 (2012) 101–108, http://dx.doi.org/10.1002/bmc.1633.
[22] J. Trottier, P. Caron, R.J. Straka, O. Barbier, Profile of serum bile acids in noncholestatic volunteers: gender-related differences in response to Fenofibrate, Clin. Pharmacol. Ther. 90 (2011) 279–286, http://dx.doi.org/10.1038/clpt.2011.124.
[23] S. Krautbauer, C. Büchler, G. Liebisch, Relevance in the use of appropriate internal standards for accurate quantification using LC-MS/MS: tauro-conjugated bile acids as an example, Anal. Chem. 88 (2016) 10957–10961, http://dx.doi.org/10.1021/acs.analchem.6b02596.
[24] H.T. Pham, K. Arnhard, Y.J. Asad, L. Deng, T.K. Felder, L.St. John-Williams, V. Kaever, M. Leadley, N. Mitro, S. Muccio, C. Prehn, M. Rauh, U. Rolle-Kampczyk, J.W. Thompson, O. Uhl, M. Ulaszewska, M. Vogeser, D.S. Wishart, T. Koal, Inter-laboratory robustness of next-generation bile acid study in mice and humans: international ring trial involving 12 laboratories, J. Appl. Lab. Med. An AACC Publ. 1 (2016) 129–142, http://dx.doi.org/10.1373/jalm.2016.020537.
[25] C. Steiner, A. von Eckardstein, K.M. Rentsch, Quantification of the 15 major human bile acids and their precursor 7α-hydroxy-4-cholesten-3-one in serum by liquid chromatography-tandem mass spectrometry, J. Chromatogr. B Anal. Technol. Biomed. Life Sci. 878 (2010) 2870–2880, http://dx.doi.org/10.1016/j.jchromb.2010.08.045.
[26] S. Jäntti, Liquid Chromatography-Tandem Mass Spectrometry Liquid Chromatography-Tandem Mass Spectrometry in Studies of Steroid Hormones and Steroid Glucuronide Conjugates in Brain and Urine, 2013.
[27] R. Thakare, H. Gao, R.E. Kosa, Y.A. Bi, M.V.S. Varma, M.A. Cerny, R. Sharma, M. Kuhn, B. Huang, Y. Liu, A. Yu, G.S. Walker, M. Niosi, L. Tremaine, Y. Alnouti, A.D. Rodrigues, Leveraging of rifampicin-dosed cynomolgus monkeys to identify bile acid 3-O-sulfate conjugates as potential novel biomarkers for organic anion-transporting polypeptidess, Drug Metab. Dispos. 45 (2017) 721–733, http://dx.doi.org/10.1124/dmd.117.075275.
[28] C. of V.M. (CVM) F.D.A. U.S. Department of Health and Human Services, Center for Drug Evaluation and Research (CDER), Bioanalytical Method Validation Guidance, 2018, pp. 25.

[29] Y. Li, X. Zhang, J. Chen, C. Feng, Y. He, Y. Shao, M. Ding, Targeted Metabolomics of Sulfated Bile Acids in Urine for the Diagnosis and Grading of Intrahepatic Cholestasis of Pregnancy, 2018, pp. 1–9, http://dx.doi.org/10.1016/j.gendis.2018.01.005.
[30] O.T. Okan, I. Denİz, N. Yayli, I.G. Şat, M. Öz, G.H. Serdar, Antioxidant Activity, Sugar content and phenolic profiling of blueberries cultivars: a comprehensive comparison, Not. Bot. Horti Agrobot. Cluj-Napoca 46 (2018) 639–652, http://dx.doi.org/10.15835/nbha46211120.
[31] C. Gälman, B. Angelin, M. Rudling, Pronounced variation in bile acid synthesis in humans is related to gender, hypertriglyceridaemia and circulating levels of fibroblast growth factor 19, J. Intern. Med. 270 (2011) 580–588, http://dx.doi.org/10.1111/j.1365-2796.2011.02466.x.